Available online at www.sciencedirect.com
ScienceDirect
Catalysis Today 122 (2007) 51–61
CATALYSIS TODAY
www.elsevier.com/locate/cattod

Photocatalysis for new energy production
Recent advances in photocatalytic water splitting reactions for hydrogen production

Masaya Matsuoka [a,*], Masaaki Kitano [a], Masato Takeuchi [a], Koichiro Tsujimaru [a], Masakazu Anpo [a,**], John M. Thomas [b]

[a] *Department of Applied Chemistry, Graduate School of Engineering, 1-1 Gakuen-cho, Sakai, Osaka 599-8531, Japan*
[b] *Davy Faraday Research Laboratory, The Royal Institution of Great Britain, 21 Albemarle Street, London W1X 4BS, UK*

Available online 6 March 2007

Abstract

Recent advances in photocatalytic water splitting reactions, especially under visible light irradiation, are reviewed here. In line with such work, the development of various unique photocatalysts including cation or anion-doped metal oxides or metal oxynitride has been introduced. Special attention is focused on the preparation of visible light-responsive TiO_2 thin films by a RF-magnetron sputtering method and their applications for the separate evolution of H_2 and O_2 from water under visible or solar light irradiation.

Keywords: Photocatalysis; Water splitting; Visible light; RF-magnetron sputtering method

1. Introduction

Sunlight in the near-infrared, visible, and ultraviolet regions radiates a tremendous amount of energy and intensity to the earth so that harnessing this solar energy would contribute significantly to our electrical and chemical needs. Thus, the application of photocatalysis to utilize such abundant and safe solar light energy is much desired and vital to sustain life. Photocatalytic reactions are usually classified into the following two categories: ''down-hill'' and ''up-hill'' reactions. In a down-hill reaction, the photon energy absorbed by a photocatalyst induces thermodynamically favored reactions such as the complete oxidation of organic compounds into CO_2 and H_2O, accompanied by a large negative change in the Gibbs free energy ($\Delta G < 0$). Such reactions have been practically applied for the degradation of toxic organic compounds in air or water with solid semiconducting photocatalysts such as TiO_2 [1,2]. On the other hand, one of the most significant ''up-hill'' reactions is the photosynthesis in plants. In this reaction, photon energy is converted into chemical energy and stored in the bonds of glucose, accompanied by a large positive change in the Gibbs free energy ($\Delta G > 0$):

$$H_2O + CO_2 \xrightarrow{h\nu} \tfrac{1}{6}(C_6H_{12}O_6) + O_2, \quad \Delta G = 480\,\mathrm{kJ/mol}$$

Since the first energy crisis in the early 1970s, much research has been devoted to the development of efficient systems that would enable the absorption and conversion of solar light into useful chemical energy resources. One of the most promising of such ''artificial photosynthesis'' reactions is the photocatalytic splitting of water to produce H_2 and O_2 under solar light:

$$H_2O \xrightarrow{h\nu} H_2 + \tfrac{1}{2}O_2, \quad \Delta G = 237\,\mathrm{kJ/mol}$$

The refinement of this up-hill reaction is greatly desired not only for the conversion and storage of solar energy but also for the clean and safe production of hydrogen since the consumption of hydrogen will be expected to increase dramatically, especially for use in fuel cells.

Theoretically, a potential difference of more than 1.23 eV between the cathodic and anodic electrodes is required for the electrochemical decomposition of water in dark conditions. This potential difference is equivalent to the energy of a photon

* Corresponding author.
** Corresponding author.
E-mail address: anpo@chem.osakafu-u.ac.jp (M. Anpo).

0920-5861/$ – see front matter
doi:10.1016/j.cattod.2007.01.042

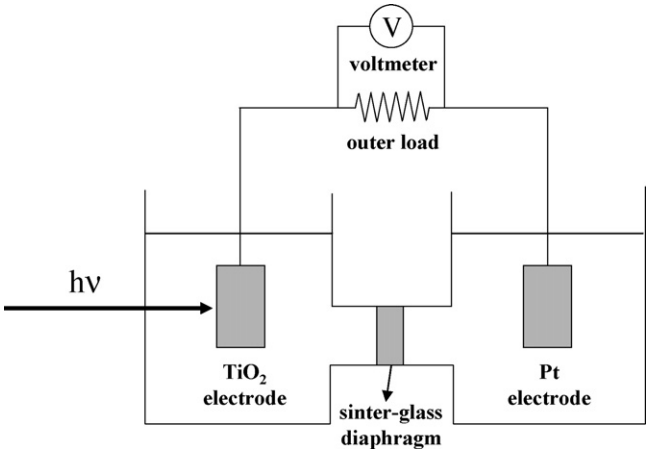

Fig. 1. Electrochemical cell in which the TiO_2 electrode is connected with a Pt electrode.

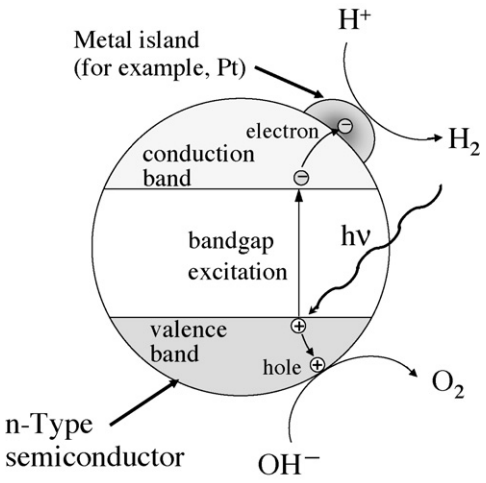

Fig. 2. Representation of semiconductor particulate systems for heterogeneous photocatalysis.

with a wavelength around 1010 nm, indicating that visible light is energetically sufficient for the decomposition of water. However, water is transparent to visible light and can be decomposed only under irradiation in vacuum ultraviolet light of wavelengths shorter than 190 nm. Since the pioneering work of Honda and Fujishima [3,4] which reported on the photodecomposition of water using semiconducting photoelectrolysis cells, many studies in the photocatalytic splitting of water have been carried out. Photoelectrolysis cells consisting of a TiO_2 electrode and Pt black electrode are connected through an external load, as shown in Fig. 1. Photo-irradiation of the TiO_2 electrode under a small electric bias led to the evolution of H_2 and O_2 at the surface of the Pt electrode and TiO_2 electrode, respectively.

$$TiO_2 \xrightarrow{h\nu} e^- + h^+$$

$$H_2O + 2h^+ \rightarrow (1/2)O_2 + 2H^+$$

$$2H^+ + 2e^- \rightarrow H_2$$

Bard's concept [5–7], which emerged in 1979, could then be applied to the design of photocatalytic systems using semiconductor particles or powders, as shown in Fig. 2. In such a Pt-loaded TiO_2 particle system (Pt/TiO_2), the TiO_2 semiconductor electrode and metal Pt counter electrode are brought into contact as a ''short-circuited'' photoelectrochemical cell. In fact, Pt/TiO_2 has not only been shown to be an efficient photocatalyst for such reactions as the complete oxidation of various organic molecules but also for the water splitting reaction into H_2 and O_2. And presently, various kinds of powdered metal oxides or metal nitrates have been found to act as efficient photocatalysts for the water splitting reaction, even under visible light.

In the present paper, the advances achieved in the photocatalytic water splitting reaction, especially under visible light, are reviewed. Special attention is focused on the preparation of visible light-responsive TiO_2 thin films by a RF-magnetron sputtering method and their application for the separate evolution of H_2 and O_2 from water.

2. Water splitting reactions under UV light irradiation

2.1. Gas phase water splitting reactions on semiconducting photocatalysts

Previously, Wagner and Somorjai have reported on a sustained H_2 evolution from gaseous water over oxide semiconductors [8–11]. Platinized $SrTiO_3$ single crystals coated with films of NaOH were used for the water splitting reaction and the H_2 production rates reached up to 1600 monolayers per hr under UV light irradiation. The evolution of H_2 and O_2 from gaseous water under UV light has also been reported by Kawai and Sakata [12] as well as Domen et al. [13], employing RuO_2/TiO_2 and $NiO/SrTiO_3$, respectively. Sato and White [14–16] have succeeded in the efficient evolution of H_2 and O_2 from gaseous water at 298 K using Pt/TiO_2 powder as the photocatalyst (Fig. 3). UV light irradiation of a Pt/TiO_2 powder coated with NaOH (of more than 7 wt.%) under saturated water vapor led to H_2 production at a rate of 20 μmol/h. The quantum efficiency of H_2 and O_2 production reached about 7% at the beginning of the reaction and no reaction was observed to proceed on the metal-free TiO_2 under identical experimental conditions. These results suggest that the loading of small amounts of Pt on the TiO_2 dramatically increased the reaction rate through an enhancement of the charge separation of the photo-formed electrons and holes by Pt deposition. It has been generally accepted that Pt loading is effective for the photocatalytic evolution of H_2 from water since the presence of Pt significantly reduces the over-potential for H_2 production [17]. However, Pt also enhances the thermal back reaction to produce H_2O from H_2 and O_2. In fact, as shown in Fig. 3, the reaction rate decreased with the accumulation of H_2 and O_2 in the gas phase and their pressures became constant ($p^{H_2}_{max} = 0.43$ Torr, $p^{O_2}_{max} = 0.20$ Torr). When UV irradiation was ceased, the pressures of H_2 and O_2 in the gas phase rapidly decreased [16]. Furthermore, it was found that the reaction rate was seen to increase with an increase in the NaOH coating from 7 to 14 wt.%, while only a small amount of H_2 was evolved

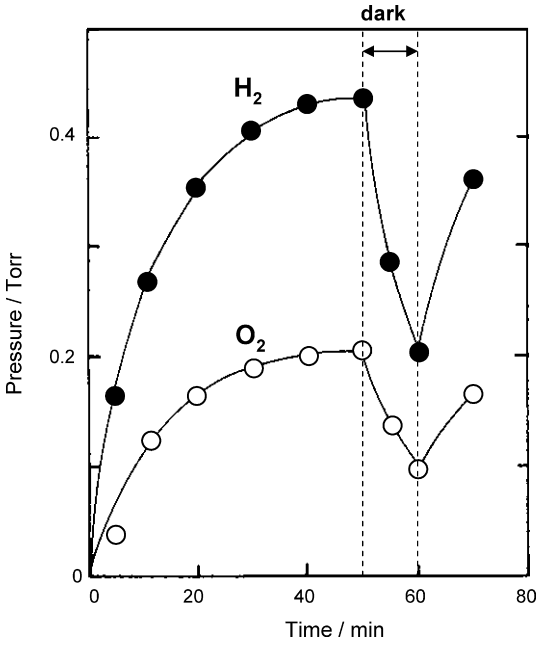

Fig. 3. Reaction time profiles of photocatalytic splitting of gas phase water on NaOH coated Pt/TiO_2 catalyst (NaOH: 7 wt.%) at 298 K.

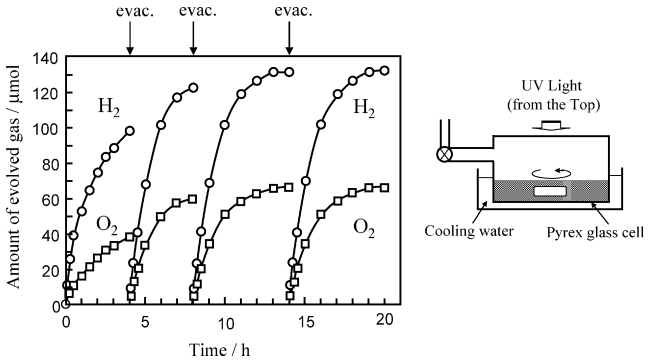

Fig. 4. Reaction time profiles of the photocatalytic splitting of water on Pt/TiO_2(P-25) (Pt: 0.1 wt.%) under UV irradiation by top-irradiation system and schematic diagram of the top-irradiation system.

without NaOH coating. The effect of the NaOH coating on the reaction rate is explained as follows. In the presence of gas phase water, thin NaOH aqueous layer is formed on the catalyst. This liquid electrolyte layer covers the Pt surface and prevents the thermal back reaction, leading to the increase in the evolution rates of H_2 and O_2. Another important role of the electrolytes is to supply water molecules to the surface of the photocatalysts, which plays a significant role in achieving a high yield for the photocatalytic decomposition of gas phase water. It has been also clarified that the back reaction rate increases with the increase of the reaction temperature, since the maximum pressures of H_2 and O_2 in the gas phase ($p_{max}^{H_2}$ and $p_{max}^{O_2}$) decrease as the reaction temperature increases. Furthermore, it has been reported that NaOH coated Rh/TiO_2 exhibits higher photocatalytic activity for the gas phase water decomposition reaction than NaOH coated Pt/TiO_2. The quantum yield ca. 29% was obtained for the reaction on the NaOH coated Rh/TiO_2 [16].

2.2. Liquid phase water splitting reactions on semiconducting photocatalysts

Pt/TiO_2 photocatalysts coated with thin aqueous NaOH solution layers can split gaseous water into H_2 and O_2. However, UV irradiation of Pt/TiO_2 suspended into sufficient amounts of water by an inner irradiation system was seen to lead to the evolution of trace amounts of H_2, since the reaction products, H_2 and O_2, react rapidly to form H_2O on the Pt surface before they escape into the gas phase through the thick water phase. However, It has been reported that, for a Pt/TiO_2 aqueous suspension system, the efficiency of the water splitting reaction strongly depends on the direction of UV irradiation. Tabata et al performed photocatalytic decomposition of water at 295 K using an top-irradiation system. The high pressure Hg lamp (250 W) was used as light source for the external-irradiation system where Photon flux was about 1.8×10^{18} photons/s after passing through the UV-cut filter ($\lambda > 350$ nm). As shown in Fig. 4, stoichiometric water decomposition can be observed only when the suspension was irradiated from the upper part of the aqueous suspension surface (top-irradiation system) [18]. In this case, H_2 and O_2 produced at the most upper part of the aqueous suspension can be easily released into the gas phase through the thin water layers without the accompanying thermal back reaction. Kominami et al have reported that nano-sized TiO_2 particles synthesized by hydrothermal crystallization in organic media (HyCOM) deposited with Pt (Pt/TiO_2(HyCOM)) exhibit high photocatalytic activity for stoichiometric water splitting reaction into H_2 and O_2 in a top-irradiation system [19]. Pt/TiO_2(HyCOM) calcined at 973 K followed by the platinum deposition showed higher photocatalytic activity (H_2 evolution rate: 40.7 μmol/h) than Pt/TiO_2(P-25) (H_2 evolution rate: 30.9 μmol/h). This high photocatalytic activity of Pt/TiO_2(HyCOM) has been ascribed to the high crystallinity of TiO_2(HyCOM), i.e., fewer crystal defects, giving a slower recombination rate of photo-formed electrons and holes. The slow recombination rate of electrons and holes on TiO_2(HyCOM) has been elucidated by femtosecond pump-probe diffuse reflectance measurements [20]. Sayama and Arakawa have reported that the addition of sodium carbonate in the aqueous suspension of Pt/TiO_2 could significantly enhance the stoichiometric evolution of H_2 and O_2 from water, even under irradiation by an inner irradiation system [21,22]. The addition of Na_2CO_3 (2 mol/l) in the aqueous suspension of Pt/TiO_2 led to the stoichiometric formation of H_2 (78 μmol/h) and O_2 (38 μmol/h) under UV irradiation, while trace amounts of H_2 (2 μmol/h) could be observed without the addition of Na_2CO_3. The rate of back reactions to form H_2O from gaseous H_2 and O_2 on Pt-loaded TiO_2 was also found to be strongly affected by the content of the reaction solutions and were seen to decrease in the following order: pure water > NaOH (aq.) > Na_2CO_3 (aq.). It was, thus, confirmed that the remarkable improvement in the reaction rate by the addition of Na_2CO_3 was caused by a decrease in the back reaction rate on the photocatalyst. The mechanism how the

addition of Na_2CO_3 increases the reaction rate of liquid phase water splitting has not been fully clarified. However, FT-IR investigations revealed that the Pt/TiO_2 catalyst is covered with several types of carbonate species during the reaction. These adsorbed carbonates are considered to play two important roles to increase the reaction rate, that is, inhibition of the thermal back reaction on Pt and effective desorption of O_2 from TiO_2 surfaces [21,22].

Moon et al. [23] have reported on titanium oxide modified with boron (B_2O_3/TiO_2) prepared by a sol–gel method which exhibited remarkable activity for the photocatalytic splitting reaction of water. Boron oxides are known to strongly interact with water molecules and become moist easily in air [23], a great advantage in the efficient splitting of water. In fact, Pt/TiO_2 modified with boron oxide ($Pt–B_2O_3/TiO_2$) exhibited a high photocatalytic activity for the splitting of water even under irradiation by an inner irradiation system. Irradiation of UV light on the $Pt–B_2O_3/TiO_2$ photocatalysts suspended in water led to the stoichiometric evolution of H_2 and O_2 in the gas phase with a good linearity against the UV irradiation time. The average rate (three runs) of H_2 evolution for the $Pt–B_2O_3/TiO_2$ was determined to be 21.9 μmol/h. These results suggest that the added boron oxide not only assists the efficient contact between water and Pt/TiO_2 but also prevents the rapid thermal back reaction between H_2 and O_2.

In addition to such Pt/TiO_2 photocatalysts, various kinds of solid photocatalysts have been reported to split pure water into H_2 and O_2. In order to enhance the activity, it is important to design photocatalysts which promote the formation of photoexcited electrons and holes as well as the transfer of these charge carriers to the adsorbed reactants. $BaTiO_4$ loaded with RuO_2 ($RuO_2/BaTiO_4$) has been reported to act as an efficient photocatalyst [24,25] for pure water splitting to produce H_2 and O_2 stoichiometrically under UV irradiation. The main structural feature of $BaTiO_4$ is the presence of a pentagonal-prism tunnel framework consisting of edge and corner-sharing of the TiO_6 octahedron. Such a twin tunnel structure facilitates a strong interaction between the $BaTiO_4$ and RuO_2 deposited as a promoter and has a favorable effect on the separation of the photoexcited charges and their transfer to the adsorbed reactants. Another interesting feature of the $BaTiO_4$ single crystal is that it has two types of largely distorted TiO_6 octahedra: one with a Ti–O distance ranging from 0.177 to 0.232 nm and the other from 0.185 to 0.216 nm. This strongly distorted TiO_6 octahedra leads to the generation of two kinds of dipole moments (D) in the pentagonal-prism tunnel: one at 5.7D and the other at 4.1D. The presence of such large dipole moments generates high internal polarization fields in the tunnel structure, facilitating the charge separation of the photo-formed electron and holes, thus, leading to the high photocatalytic activity of $RuO_2/BaTiO_4$, as shown in Fig. 5.

$K_4Nb_6O_{17}$ has been reported to have a Perovskite structure [26–28], thus, showing characteristic activity for the photocatalytic splitting of water into H_2 and O_2. $K_4Nb_6O_{17}$ is a layered compound in which the NbO_6 units are connected by oxygen atoms in a corrugated two-dimensional layered structure. Moreover, K^+ can be replaced by various cations

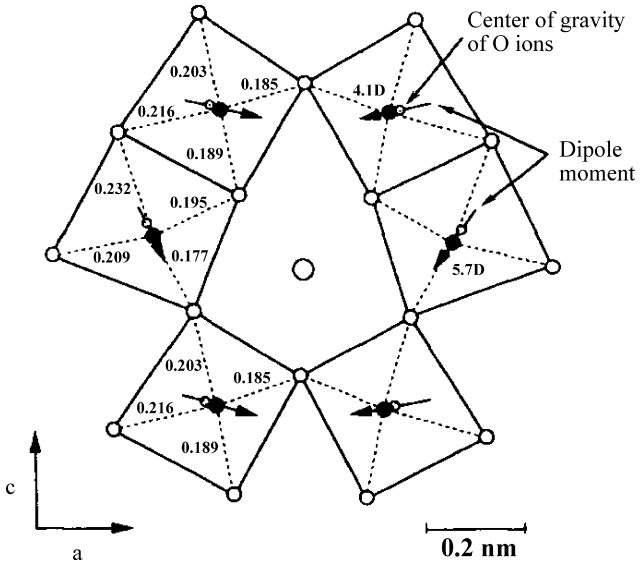

Fig. 5. A pentagonal-prism tunnel structure of $BaTi_4O_9$. Filled circle: Ti^{4+}; small circle: O^{2-}; large circle: Ba^{2+}; shaded circle: center of gravity. The arrows indicate dipole moments. The numbers express the Ti–O bond length in nm.

and, in this structure, two types of interlayers exist alternatively: interlayer I has the capacity to adsorb water molecules while interlayer II is not hydrated under ambient conditions. The photocatalytic reactivity for the splitting of pure water over $K_4Nb_6O_{17}$ and photocatalysts loaded with small amounts of NiO are summarized in Table 1. A marked increase in the photocatalytic activity and stoichiometric evolution of H_2 and O_2 are observed when $K_4Nb_6O_{17}$ is loaded with NiO. The photocatalytic reactivity was also found to strongly depend on the pretreatment conditions. For the photocatalysts reduced with H_2 at 773 K, the activity increased significantly, indicating that this pretreatment is instrumental for the efficient photocatalytic splitting of water.

The structural changes in the catalysts brought about by such pretreatment conditions were monitored by XPS and XAFS investigations. XPS analysis revealed that Ni does not exist on the surface during the pretreatment period, indicating that most of the Ni are located inside $K_4Nb_6O_{17}$. Moreover, EXAFS measurements revealed that Ni exists in the form of NiO-like fine particles before H_2 reduction. When the catalyst was reduced at 773 K by H_2, the NiO-like fine particles were completely transformed into Ni metal. Interestingly, most of the Ni remains in the metallic state, even after it has been reoxidized at 473 K in the final step of the activation treatment. This suggests that reoxidation with O_2 oxidizes only the Ni attached to the outer surfaces of $K_4Nb_6O_{17}$ but not the Ni existing inside. When considering that Ni^{2+} is exchanged with K^+ ions only within interlayer I [29], the ultrafine particles of NiO prepared can also be thought to exist within the interlayer space I as well. The structure and proposed mechanism of the decomposition of water over Ni-loaded $K_4Nb_6O_{17}$ are shown in Fig. 6. First, the layers of the niobate sheets absorb photons to produce excited electrons and holes. The electrons are then transferred to the Ni particles in interlayer I and reduce H^+ to H_2 while the site for O_2 evolution is thought to be interlayer II

Table 1
Photocatalytic activities over $K_4Nb_6O_{17}$ and NiO–$K_4Nb_6O_{17}$ after pretreatment

Catalysts	Pretreatment	H_2O		CH_3OH_{aq}[a] H_2 (μmol/h)	$AgNO_{3aq}$[b] O_2 (μmol/h)
		H_2 (μmol/h)	O_2 (μmol/h)		
$K_4Nb_6O_{17}$	Untreated	5	0	177	10
	R773	5	1		
	R773-O473	8	1		
NiO (0.1 wt.%)–$K_4Nb_6O_{17}$	Untreated	4	1	667	2
	R773	55	28	1593	7
	R773-O473	77	37	1300	9

[a]MeOH:H_2O = 1:30 (v/v); [b]0.01 mol/l.; catalyst, 1 g; solution, 300 ml; light source, high-pressure mercury lamp (450 W); reaction cell, inner irradiation reaction cell. R773: reduction under H_2 at 773 K. O473: oxidation under O_2 at 473 K.

where Ni particles do not exist. In this mechanism, the H_2-forming sites are completely separated from the O_2-forming sites by niobic acid sheets, preventing any reverse reaction on the Ni metal. Moreover, the products in the gas phase cannot effectively diffuse back into the interlayer space. This photocatalyst is, thus, regarded as a ''two-dimensional photocatalyst'' which makes effective use of the surface and bulk of niobium acid sheets to split water molecules intercalated between two opposing layers.

Kato et al. have reported on NiO-loaded $NaTaO_3$ (NiO/$NaTaO_3$) which showed high photocatalytic activity for pure water splitting into H_2 and O_2 stoichiometrically under UV light [30]. Here, NiO small particles were deposited on the surface of $NaTaO_3$ by impregnation method. The photocatalytic activity of NiO/$NaTaO_3$ of a Perovskite-like structure was enhanced dramatically by the doping of La and the prepared NiO/$NaTaO_3$:La exhibited nine times higher activity than that of non-doped NiO/$NaTaO_3$. The maximum apparent quantum yield of the NiO/$NaTaO_3$:La photocatalyst was 56% at 270 nm. Electron microscopic observations revealed that the particle sizes of the $NaTaO_3$:La crystals (0.1–0.7 μm) were smaller than the non-doped $NaTaO_3$ crystals (2–3 μm) and that characteristic ordered surface nanostructure with many characteristic steps was created by the doping of lanthanum. The small particle size and high crystallinity was advantageous in increasing the probability for reactions of the photo-formed electrons and holes with the water molecules. Concerning the effect of the addition of lanthanum, the XRD and energy dispersive X-ray investigations revealed that the majority of doped lanthanum localized near the surface and was substituted for sodium ions. From the results, it has been considered that the lanthanum localizing near the surface prevented the crystal growth, resulting in the formation of fine particles of $NaTaO_3$ and the creation of the characteristic nanoscale step structure. It was also concluded that the high activity of NiO/$NaTaO_3$:La could be ascribed to the suitable conduction band (CB) level (−1.06 eV versus NHE) for the photogenarated electrons to transfer to the NiO co-catalyst (CB level: −0.96 eV versus NHE) [31].

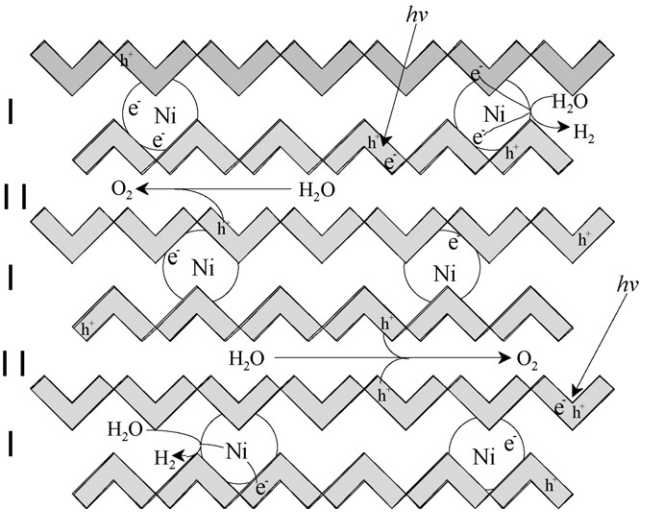

Fig. 6. Schematic structure of the active NiO (0.1 wt.%)–$K_4Nb_6O_{17}$ photocatalyst and the reaction mechanism of the splitting of H_2O into H_2 and O_2.

3. Water splitting reactions under visible light irradiation

3.1. Water splitting reactions on cation doped metal oxide photocatalysts

Various kinds of semiconducting metal oxides have been reported to act as efficient photocatalysts to split gaseous or liquid phase water into H_2 and O_2 under UV light irradiation. However, most of metal oxide photocatalysts are unable to split pure water under visible light. This is mainly due to the fact that the smaller the band gap energy of the metal oxide becomes, the more positively its conduction band edge shifts [32]. Thus, the conduction band edge of metal oxides having a small band gap energy tends to locate quite close to the redox potential of H^+/H_2 redox couple (0 eV versus NHE), in some cases, locate more positive than the redox potential of H^+/H_2, losing their ability to reduce H^+ into H_2. However, much work has been done to develop visible light-responsive metal oxide photocatalysts such as the chemical doping of TiO_2 with transition metals ions or oxides [33]. Although TiO_2 chemically doped with metal ions could, in fact, induce visible light response, these catalysts showed limitations in sufficient reactivity for practical applications. When metal ions or oxides are incorporated into TiO_2 by a chemical doping method, the impurity energy levels formed in the band gap of TiO_2 may cause an increase in the

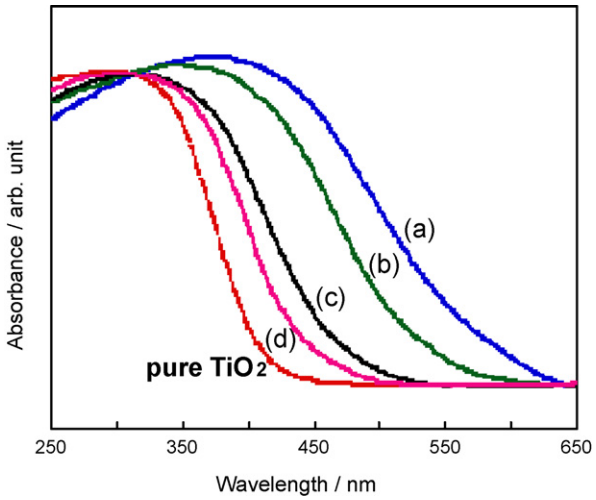

Fig. 7. The diffuse refrectance UV–vis absorption spectra of TiO_2 photocatalysts implanted with V (a), Cr (b), Fe (c), Ni ions (d) with the same amount of 1.33 μmol/g cat.

recombination between the photo-formed electrons and holes [34].

Anpo et al. [35–42] have reported on TiO_2 photocatalysts capable of the absorption of visible light up to 550 nm by applying an advanced metal ion-implantation method to modify the electronic properties of the semiconductors by bombarding them with various metal ions accelerated by high voltage. The absorption band of the TiO_2 photocatalysts implanted with metal ions, such as Cr, V, Fe, Ni, etc., was found to shift to visible light regions, the extent of the red shift depending on the amount and type of metal ions implanted, as shown in Fig. 7. ESCA and XAFS measurements have indicated that the implanted metal ions are present deep inside the TiO_2 bulk and are located in the lattice position of TiO_2 in place of the Ti^{4+} ions. These results suggest that the chemical interactions of such highly dispersed metal ions with the TiO_2 moieties causes a modification in the band structures of TiO_2, enabling the absorption of visible light. The photocatalytic activity of Pt-loaded TiO_2 thin film photocatalysts implanted with metal ions such as Cr and V (Pt/TiO_2–Cr and Pt/TiO_2–V) were also investigated for the evolution of H_2 from aqueous solution involving methanol as a sacrificial reagent. Here, visible light irradiation was carried out with a 500 W Xe arc lamp through a quartz cell filled with $NaNO_2$ solution to pass only visible light ($\lambda > 400$ nm). H_2 was evolved when the Pt/TiO_2–Cr and Pt/TiO_2–V thin films were irradiated under visible light longer than 400 nm, while no H_2 evolution could be observed with the non-implanted Pt-loaded TiO_2 thin films.

Kudo et al. reported that TiO_2 co-doped with Ni^{2+} and Ta^{5+} (Ni–Ta/TiO_2) exhibited photocatalytic activity under visible light irradiation ($\lambda > 440$ nm) for O_2 evolution from an aqueous silver nitrate solution [43]. Here, Ni^{2+} or Ta^{5+} ions are doped into the TiO_2 and $SrTiO_3$ lattice by the solid-state-reaction at 1423 K. XRD peaks of TiO_2 shifted to the lower angles by the Ni^{2+} doping (Ni/TiO_2), suggesting that Ni^{2+} ion (0.830 Å) substitutes Ti^{4+} ion (0.745 Å) at the Ti^{4+} site. Furthermore, it was found that the substitution of Ni^{2+} is enhanced by the co-doping of Ta^{5+} which compensate the small positive valence of Ni^{2+} within TiO_2 matrices, as evidenced by the larger shift of the XRD peaks observed for Ni–Ta/TiO_2 than Ni/TiO_2. Ni/TiO_2 shows UV–vis absorption band up to 500 nm and the intensity of the absorption band in the visible light region was dramatically enhanced by the co-doping of Ta^{5+}. Ni/TiO_2 exhibited photocatalytic activity for O_2 evolution from an aqueous silver nitrate solution under visible light irradiation ($\lambda > 440$ nm), while the O_2 evolution rate was remarkably enhanced by the co-doping of Ta^{5+}. It was also found that $SrTiO_3$ co-doped with Ni^{2+} and Ta^{5+} (Ni–Ta/$SrTiO_3$) showed photocatalytic activity for H_2 evolution from an aqueous methanol solution under visible light irradiation ($\lambda > 420$ nm) [43]. It has been reported that 3d orbitals of Ni^{2+} form an electron donor level at a more negative potential than the O 2p band [43]. In fact, in the case of Ni^{2+}doped ZnS photocatalyst, visible light absorption occurs due to the electronic transition from a donor level formed by Ni^{2+} 3d orbitals in the forbidden band to the conduction band [43]. Thus, these visible light responses of TiO_2 or $SrTiO_3$ co-doped with Ni^{2+} and Ta^{5+} can be attributed to the charge transfer transition from the electron donor levels formed by the 3d orbitals of doped Ni^{2+} to the conduction bands of the host materials as shown in Fig. 8.

These TiO_2 photocatalysts doped with various transition metal ions could absorb visible light and split water only in the presence of a sacrificial reagent such as methanol or silver nitrate. Zou et al. have reported that indium–tantalum-oxide doped with nickel ($In_{0.9}Ni_{0.1}TaO_4$) and supported with NiOx or RuO_2 as the promoter induced the direct splitting of water into stoichiometric amounts of oxygen and hydrogen under visible light irradiation ($\lambda > 420$ nm), where the partially filled Ni 3d shell plays an important role in the modification of the electronic properties of $InTaO_4$ [44]. These findings are supported by the appearance of an absorption band at 420–520 nm in the Ni-doped compounds. The quantum yield of the direct splitting of water on $In_{0.9}Ni_{0.1}TaO_4$ at 402 nm was estimated to be 0.66%.

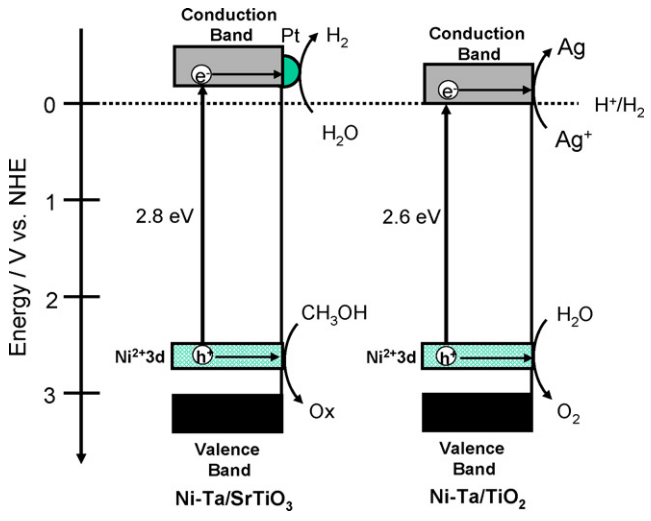

Fig. 8. Schemes of photocatalytic evolution of H_2 and O_2 on Ni–Ta/TiO_2 and Ni–Ta/$SrTiO_3$ under visible light irradiation.

3.2. Water splitting reactions on anion doped metal oxides or metal oxynitrides

Recently, many studies have been devoted to the development of visible light-responsive TiO_2 by doping various kinds of anions such as N [45,46], S [47,48] or C [49–51] as a substitute for oxygen in the TiO_2 lattice. For these anion doped TiO_2 photocatalysts, the mixing of the p states of doped anion (N, S and C) with the O 2p states was reported to shift the valence band edge upwards to narrow the band gap energy of TiO_2. Under visible light, these materials exhibited photocatalytic activity for the degradation of 2-propanol [48], acetaldehyde [45] and acetone [50]. However, no activity was observed for pure water splitting, although the conduction and valence bands of these materials have enough potential for the reduction of H^+ into H_2 and the oxidation of water to O_2, respectively. One of the reasons of these phenomena can be attributed to the large over-potential of H_2 or O_2 evolution reactions on the surface of these photocatalysts. However, it has since been reported that metal oxynitrides or metal nitrides can be efficient photocatalysts for the stoichiometric splitting of H_2O into H_2 and O_2 under visible light irradiation.

Abe et al have succeeded in the direct splitting of pure water into stoichiometric amounts of H_2 and O_2 under visible light irradiation ($\lambda > 420$ nm) using a Z-scheme system which consists of Pt-loaded TaON (Pt–TaON) for H_2 evolution, Pt-loaded WO_3 (Pt–WO_3) for O_2 evolution and a IO_3^-/I^- redox mediator [52], as shown in Fig. 9. The reaction mechanism can be explained as follows: water is reduced into H_2 and I^- is oxidized into IO_3^- over the Pt–TaON while, at the same time, water is oxidized into O_2 and IO_3^- is reduced into I^- over the Pt–WO_3. Water could, thus, be decomposed into H_2 and O_2 without the consumption of the IO_3^- and I^- ions.

Recently, Maeda et al have reported that the overall splitting of water under visible light can proceed on a solid solution of gallium and zinc nitrogen oxide, $(Ga_{1-x}Zn_x)(N_{1-x}O_x)$, modified with nanoparticles of a mixed oxide of rhodium and chromium [53]. The stoichiometric evolution of hydrogen and oxygen was observed under visible light ($\lambda > 400$ nm) on the catalyst. Furthermore, it was found that the quantum efficiency for the reaction decreases with an increase in the wavelength of the irradiated light and that the longest wavelength suitable for overall water splitting coincides with the absorption edge of the $(Ga_{1-x}Zn_x)(N_{1-x}O_x)$ solid solution. The quantum efficiency at 420–440 nm was determined to be about 2.5%. Density functional theory (DFT) calculations indicated that the bottom of the conduction band for GaN:ZnO is mainly composed of 4s and 4p orbitals of Ga, while the top of the valence band consists of N2p orbitals followed by Zn3d orbitals, leading to a p-d repulsion for the valence band maximum and resulting in a narrowing of the band gap.

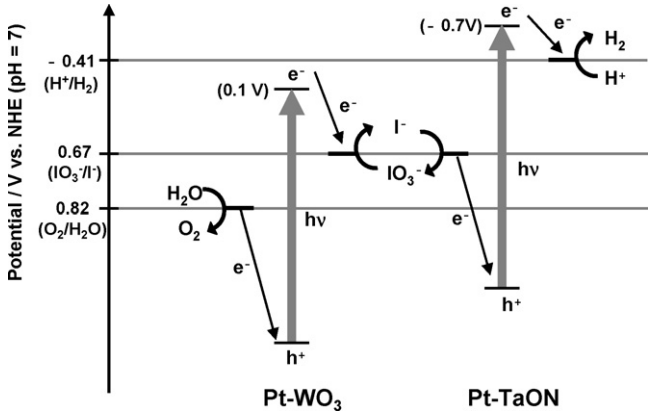

Fig. 9. Proposed reaction mechanism for water splitting over Pt–TaON and Pt–WO_3 with an IO_3^-/I^- shuttle redox mediator under visible light irradiation ($\lambda > 420$ nm).

3.3. Separate evolution of H_2 and O_2 from water under visible light irradiation

The photocatalytic splitting of water under visible light irradiation is a greatly desired reaction system for the production of H_2. However, powdered photocatalysts always produce a gas mixture of H_2 and O_2 in such a splitting reaction and, thus, a separation process for the gas mixture is required before the H_2 can be effectively utilized. Construction of a photocatalytic system enabling the separate evolution of H_2 and O_2 from water under visible light irradiation is, therefore, of vital interest.

Matsumura et al. have reported that the separate evolution of H_2 and O_2 could be achieved by combining two photocatalytic reactions on suspended TiO_2 powders using a two-compartment cell equipped with platinum electrodes and a cation-exchange membrane, as shown in Fig. 10 [54]. When both compartments were irradiated by UV light, O_2 was produced on the rutile-TiO_2 suspended in the Fe^{3+}/Fe^{2+} redox mediator solution and H_2 was evolved on the Pt-loaded anatase-TiO_2 in the Br_2/Br^- redox mediator solution. The Br_2 formed in the H_2 evolution system showed enough potential for the oxidation of Fe^{2+} in the O_2 evolution system, thus, enabling the separate evolution of H_2 and O_2 from water under UV light irradiation.

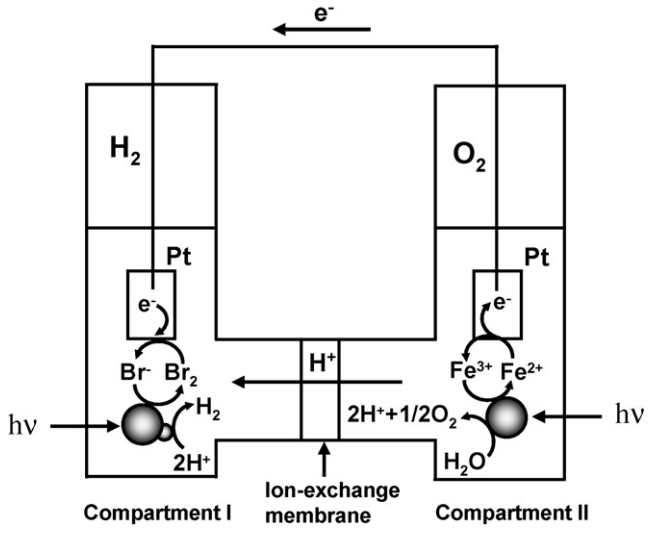

Fig. 10. Schematic diagram of the photocatalytic splitting of water using a two-compartment cell equipped with platinum electrodes and a cation-exchange membrane.

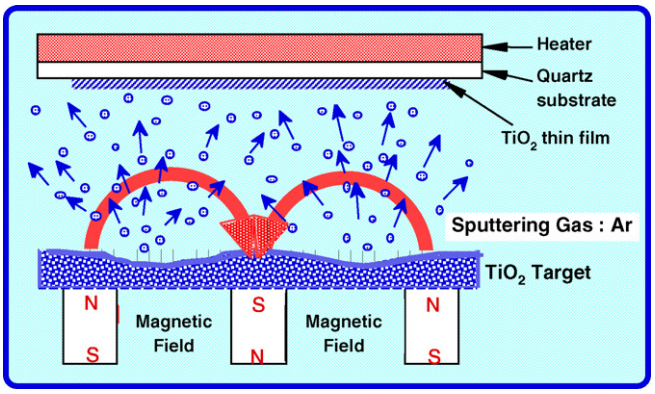

Fig. 11. Schematic diagram of RF-magnetron sputtering method.

Recently, Anpo et al. have succeeded in the preparation of visible light-responsive TiO_2 thin films for the separate evolution of H_2 and O_2 from water under visible light irradiation by applying a RF-magnetron sputtering (RF-MS) method, as shown in the schematic diagram in Fig. 11 [55–63]. The system is equipped with a substrate (quartz or Ti foil) center positioned in parallel just above the source material, the calcined TiO_2 plate. The target-to-substrate distance (D_{ts}) was fixed at the value between the range of 70–90 mm. The calcined TiO_2 plate is sputtered by Ar plasma by inducing a RF power of 300 W in Ar atmosphere and the TiO_2 thin film is prepared on the quartz or Ti metal foil substrate mounted on the heater. The substrate temperature (T_S) was held at a fixed degree between the range of 473–873 K. Pt deposition was also performed by the RF-MS method under a substrate temperature of 298 K.

Fig. 12(a, b and d) shows the effect of T_S on the UV–vis transmission spectra of TiO_2 thin films prepared on a quartz substrate with D_{ts} of 80 mm. The thickness for all films was fixed at around 1.2 μm. These spectra are characterized by the well-known oscillations appearing when a transparent thin film of a material of high refractive index is deposited on a lower refractive index substrate. TiO_2 thin films prepared at Ts of

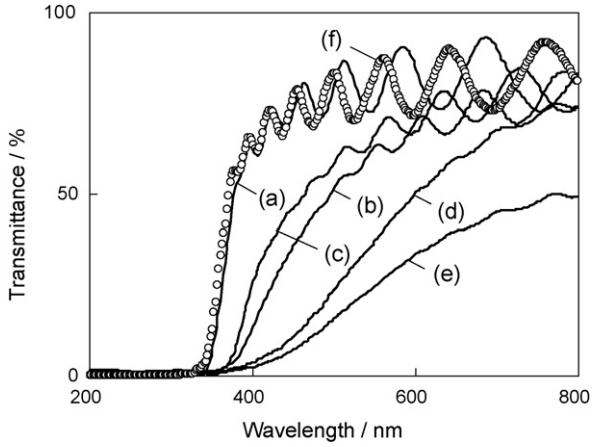

Fig. 12. UV–vis transmission spectra of (a–e) TiO_2 thin films prepared on quartz substrates under various substrate temperatures (T_S) and target-to-substrate distances (D_{ts}) in Ar atmosphere and (f) TiO_2 thin films prepared on quartz substrates prepared in Ar + O_2 atmosphere (Ar:O_2 = 5:1). T_S (K): (a) 473; (b) 673; (c–f) 873; D_{ts} (mm): (c) 90; (a, b, d and f) 80; (e) 70.

473 K with D_{ts} of 80 mm (denoted as UV–TiO_2-(473,80)) have no absorption in wavelengths longer than 380 nm, while the TiO_2 thin films prepared at 673 K (vis-TiO_2-(673,80)) and at 873 K (vis-TiO_2-(873,80)) are yellow-colored and exhibit considerable absorption in wavelengths region longer than 380 nm, enabling the absorption of visible light [56–63]. Among these three types of TiO_2 thin films, vis-TiO_2-(873,80) exhibited an adsorption edge at the longest wavelength regions around 600 nm. Thus, it has been revealed that the precise control of the substrate temperature enables the development of unique visible light-responsive TiO_2 thin film photocatalysts, the efficiency of visible light absorption increasing with as increase in the substrate temperature. It should be noted that the coexistence of O_2 with Ar in the sputtering chamber leads to the formation of UV light-responsive TiO_2 thin films (Fig. 12(f)), regardless of the substrate temperature ($T_S > 673$ K) during the sputtering process. This suggests that TiO_2 deposition under pure Ar gas without any trace of O_2 is also one of the important factors in the preparation of vis-TiO_2 thin film photocatalysts. Furthermore, XRD investigations revealed that UV-TiO_2-(473,80) and vis-TiO_2-(673,80) have an anatase crystalline structure while vis-TiO_2-(873,80) mainly consists of rutile crystalline phases.

To clarify the origin of visible light absorption of vis-TiO_2-(873,80), SIMS and TEM measurements were performed. The secondary ion intensity due to ^{18}O for the UV-TiO_2-(473,80) exhibits the stoichiometric O/Ti value of 2.00 independent of the depth from the TiO_2 surface, while in the case of vis-TiO_2-(873,80), O/Ti value gradually decreases from the top surface (O/Ti ratio: 2.00 ± 0.01) to the inside bulk (1.93 ± 0.01) showing distinct contrast to UV-TiO_2-(473,80) [56–62]. It could thus be suggested that the unique declined composition of vis-TiO_2 thin films with an anisotropic structure causes a significant perturbation in the electronic structure of the TiO_2, enabling the absorption of visible light. As shown in Fig. 13, cross-sectional TEM observations revealed that vis-TiO_2-(873,80) consists of large columnar crystals growing perpendicular to the substrate and the surface of the columnar crystals are covered with a stoichiometric TiO_2 phase. Such a stable surface phase of the columnar crystals worked as passive phase and could protect the slightly reduced TiO_2 phases inside the

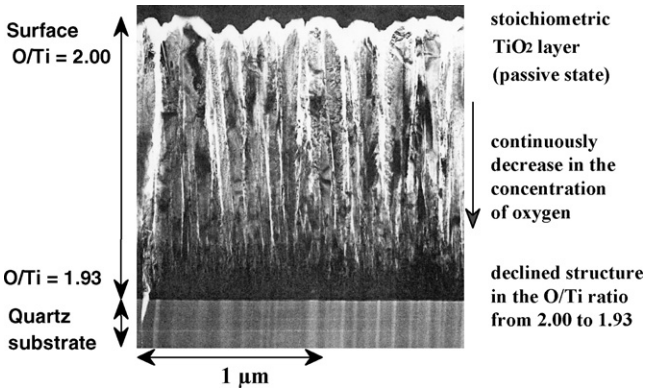

Fig. 13. Cross-sectional TEM image of the vis-TiO_2-(873,80) thin film photocatalyst.

Table 2
Quantum yields for H_2 and O_2 evolution from aqueous solutions of methanol and silver nitrate on TiO_2 thin films under UV and visible light irradiation

Photocatalyst	Quantum yield (%)			
	λ = 360 nm		λ = 420 nm	
	H_2[a]	O_2[b]	H_2[a]	O_2[b]
Pt/UV-TiO_2-(473,80)	26.2	12.6	0.00	0.00
Pt/vis-TiO_2-(673,80)	27.2	38.0	0.13	0.85
Pt/vis-TiO_2-(873,70)	5.2	8.2	0.05	0.18
Pt/vis-TiO_2-(873,80)	34.2	60.0	1.25	2.43
Pt vis-TiO_2-(873,90)	26.5	32.8	0.10	0.58

[a] From 50 vol.% aqueous methanol solutions.
[b] From 0.05 M aqueous silver nitrate solution.

bulk from complete oxidation. In fact, the physical and chemical properties of vis-TiO_2-(873,80) scarcely changed even after the calcination in O_2 at 773 K. The photocatalytic activity of Pt loaded vis-TiO_2-(873,80) (Pt/vis-TiO_2-(873,80)) was investigated under visible light irradiation. Visible light irradiation (λ = 420 nm) of Pt/vis-TiO_2-(873,80) in the aqueous methanol solution (50% methanol solution) led to the evolution of H_2, with quantum yield of 1.25 (λ = 420 nm) as shown in Table 2, showing its responsiveness to visible light, while Pt/UV-TiO_2-(473,80) exhibit no activity under same reaction condition. Furthermore, it was found that Pt/vis-TiO_2-(873,80) shows higher activity than Pt/UV-TiO_2-(473,80) under UV light irradiation (λ = 390 nm) as well. The O_2 evolution reaction was also examined in an aqueous silver nitrate solution (0.05 M silver nitrate solution) in which the following stoichiometric reaction takes place: $4Ag^+ + 2H_2O \rightarrow 4Ag^0 + O_2 + 4H^+$. The Pt/vis-$TiO_2$-(873,80) exhibited higher activity for O_2 evolution than Pt/UV-TiO_2-(473,80), especially under visible light irradiation (λ = 420 nm) with quantum yield of 2.43. These results clearly show that the RF-MS method enables the development of novel and unique visible light-responsive TiO_2 thin film which can efficiently absorb both UV and visible light as well as exhibit high photocatalytic performance. UV–vis transmittance spectra as well as the photocatalytic activity of visible light–responsive TiO_2 thin films prepared at 873 K (vis-TiO_2-(873)) were found to be dramatically affected by D_{ts}. The absorption spectra of vis-TiO_2-(873) shifted toward longer wavelength regions with the decrease in D_{ts} from 90 to 70 mm (Fig. 12(c–e)). Furthermore, it was found that both of the H_2 and O_2 evolution rate under visible light irradiation on Pt–vis-TiO_2-(873) remarkably increased with the decrease in D_{ts} from 90 to 80 mm (Table 2). This enhanced photocatalytic activity can be ascribed to the large shift of the absorption edge of vis-TiO_2-(873,80) toward visible light region as compared to vis-TiO_2-(873,90). Further decrease in D_{ts} led to the drastic decrease in the H_2 and O_2 evolution rate under both UV and visible light irradiation, in spite of the strong visible light absorption of vis-TiO_2-(873,70). The typical absorption band of vis-TiO_2-(873,70) in the range of 600–800 nm can be ascribed to the Ti^{3+} centers [64] formed by the strong attack of the high energy sputtered atoms or Ar plasma around the TiO_2 target. In fact, an ESR signal due to the Ti^{3+} centers ($g_\perp$ = 1.975 and $g_{||}$ = 1.940) [65] was observed for vis-TiO_2-(873,70). Thus formed Ti^{3+} may act as the recombination centers of photo-formed electrons and holes, leading to the decrease in the photocatalytic activity of Pt–vis-TiO_2-(873,70). The control of the D_{ts} during the simple one-step TiO_2 deposition process was, thus, found to be one of the major contributing factors in synthesizing highly active visible light-responsive thin films.

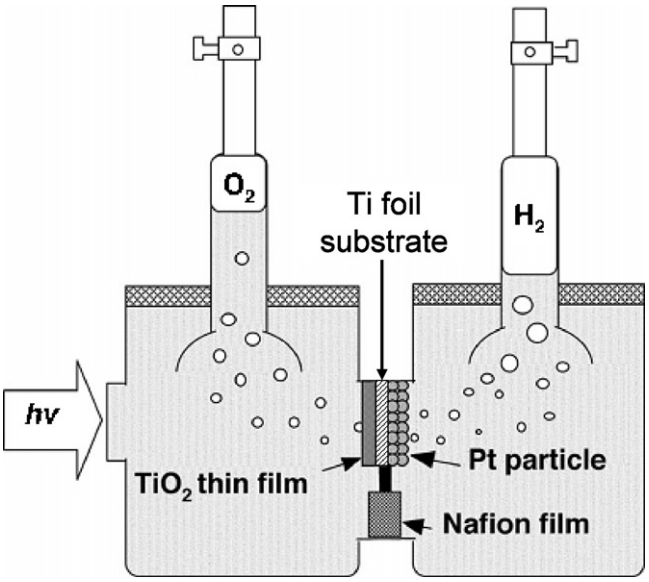

Fig. 14. H-type glass container for the separate evolution of H_2 and O_2 using a TiO_2 thin film device (vis-TiO_2-(873,80)/Ti/Pt). TiO_2 side, 1 N NaOH aq., Pt side, 1 N H_2SO_4 aq.

Separate evolution of H_2 and O_2 from water was investigated under visible light as well as solar light irradiation by using TiO_2 thin film device prepared by an RF-MS method. TiO_2 thin film device (vis-TiO_2-(873,80)/Ti/Pt) consists of the Ti foil with 50 μm thickness deposited on one side with vis-TiO_2-(873,80) thin film and on the other side with Pt. Thus prepared TiO_2 thin film device is mounted on a H-type glass container, as shown in Fig. 14, separating the two aqueous solutions. The TiO_2 side of the thin film device was immersed into 1.0 N NaOH aqueous solution and the Pt side being immersed into 1.0 N H_2SO_4 aqueous solution in order to add a small chemical bias between the two aqueous solutions. The visible light irradiation (λ > 450 nm) of the vis-TiO_2-(873,80)/Ti/Pt mounted in an H-type glass container leads to the stoichiometric evolution of H_2 and O_2 separately with good linearity against the irradiation time, while the evolutions of trace amounts of H_2 and O_2 were observed for UV-TiO_2-(473,80)/Ti/Pt (Fig. 15) [60,61]. Fig. 16 shows the effect of the irradiation time of sunlight from the sunlight-gathering system (Laforet Engineering, XD-50D) on the amounts of evolved H_2 and O_2. Sunlight irradiation of vis-TiO_2-(873,80)/Ti/Pt device successfully led to the separate evolution of H_2 and O_2, stoichiometrically. The decline observed in the evolution rate of H_2 and O_2 in the late afternoon (2:00 p.m.) can be attributed to a decline in the intensity of the sunlight [58,61,62]. It should be noted that reaction hardly proceeded on the UV-TiO_2-(473,80)/Ti/Pt device under sunlight irradiation. Furthermore, as shown in

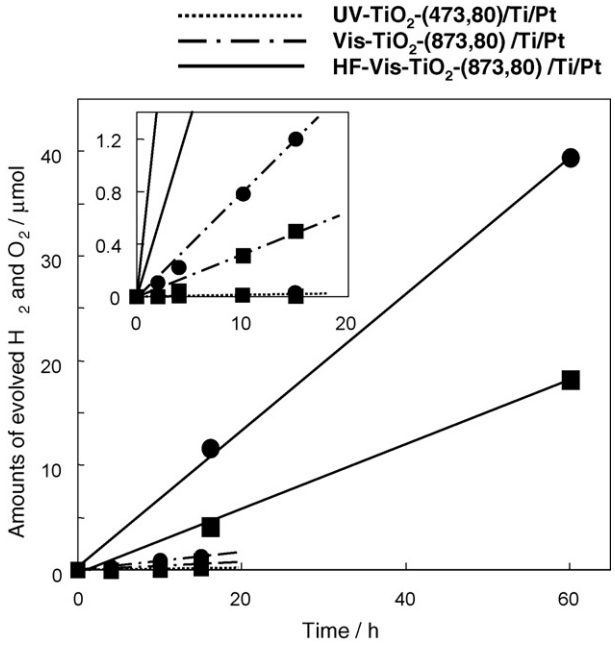

Fig. 15. Separate evolution of (●) H_2 and (■) O_2 on TiO_2 thin film devices under visible light irradiation ($\lambda > 450$ nm) in an H-type glass container. Inset shows the expanded plots in the reaction time region from 0 to 20 h. (TiO_2 film thickness: 3.0 mm). TiO_2 side, 1 N NaOH aq., Pt side, 1 N H_2SO_4 aq.

Fig. 17, reasonable photocurrent transient response was observed under sunlight irradiation for vis-TiO_2-(873,80) but not for UV-TiO_2-(473,80), showing good parallel relationship between the photocatalytic activity and the anodic photocurrents of TiO_2 thin films [63].

The effect of chemical etching on the photocatalytic activity of TiO_2 thin film device was also investigated. TiO_2 thin film device (vis-TiO_2-(873,80)/Ti/Pt) was chemically etched by immersing it into the 0.045% HF aqueous solution for 60 min to obtain HF–vis-TiO_2-(873,80)/Ti/Pt thin film device. As shown in Fig. 15, HF treatment led to the drastic increase of the

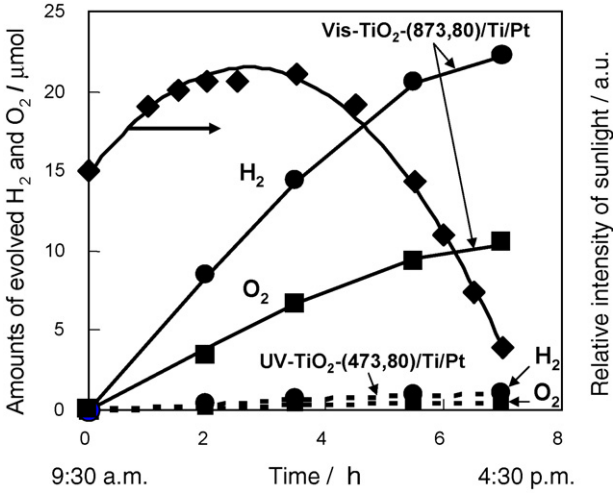

Fig. 16. Separate evolution of H_2 and O_2 on TiO_2 thin film devices under sunlight irradiation in a H-type glass container. TiO_2 side, 1 N NaOH aq., Pt side, 1 N H_2SO_4 aq.

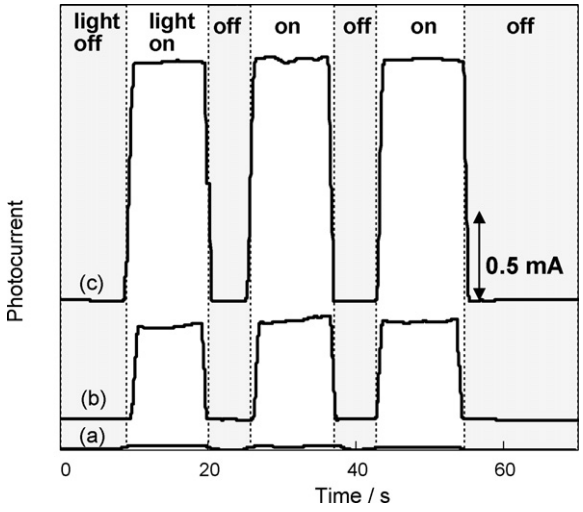

Fig. 17. Photocurrent transient curves of (a) UV-TiO_2-(473,80), (b) vis-TiO_2-(873,80) and (c) HF–vis-TiO_2-(873,80) under sunlight irradiation at +1.0 V vs. SCE in 0.1 M $HClO_4$ aqueous solution.

photocatalytic activity of vis-TiO_2-(873,80)/Ti/Pt under visible light irradiation ($\lambda > 450$ nm). Furthermore, HF–vis-TiO_2-(873,80) exhibited higher photocurrent than vis-TiO_2-(873,80) under sunlight irradiation, while photocurrent response was hardly observed for UV-TiO_2 (Fig. 17). These results clearly show that HF–vis-TiO_2-(873,80) thin films can act as an efficient photocatalyst for the separate evolution of H_2 and O_2 from H_2O under visible light irradiation ($\lambda > 450$ nm) as well as sunlight irradiation. It was, thus, demonstrated that the surface etching of TiO_2 thin films by HF treatment is an effective method in improving the photocatalytic reactivity as well as photoelectrochemical performance.

Thus, novel photocatalytic system which enables the separate evolution of H_2 and O_2 from water under sunlight irradiation has been achieved by using visible light-responsive TiO_2 thin film devices. This photocatalytic system contrasts with Pt-loaded TiO_2 nanoparticle catalysts which yield the mixture of H_2 and O_2 from water and exhibit relatively low activity because of the inevitable back reaction to form water from H_2 and O_2 on the Pt sites.

4. Conclusions

Recently, significant advances have been achieved in the design and development of unique photocatalytsts which can split water into H_2 and O_2. Various metal oxide catalysts having unique crystal structure such as $K_4Nb_6O_{17}$ and NiO/$NaTaO_3$ were found to be efficient photocatalysts for the stoichiometric water splitting reaction, where the effective charge separation of the photo-formed electrons and holes and their efficient reaction with water can be realized. It has been demonstrated that various preparation methods such as an cation- or anion-doping into metal oxides or RF magnetron sputtering method enable the preparation of unique photocatalysts which are active for the water splitting reaction even visible light irradiation. Especially, it has been demonstrated that the H-type glass container equipped with visible light-responsive TiO_2 thin

film devices prepared by RF magnetron sputtering method allow the stoichiometric and separate evolution of H_2 and O_2 from water even under solar beam irradiation.

References

[1] A. Fujishima, T.N. Rao, D.A. Tryk, J. Photochem. Photobiol. C 1 (2000) 1.
[2] D.F. Ollis, H. Al-Ekabi, Photocatalytic Purification and Treatment of Water and Air, Elsevier, Amsterdam, 1993.
[3] A. Fujishima, K. Honda, Bull. Chem. Soc. Jpn. 44 (1971) 1148.
[4] A. Fujishima, K. Honda, Nature 238 (1972) 37.
[5] A.J. Bard, J. Photochem. 10 (1979) 59.
[6] A.J. Bard, Science 207 (1980) 139.
[7] A.J. Bard, J. Phys. Chem. 86 (1982) 172.
[8] F.T. Wagner, S. Ferrer, G.A. Somorjai, Surf. Sci. 101 (1980) 462.
[9] F.T. Wagner, G.A. Somorjai, Nature 285 (1980) 559.
[10] F.T. Wagner, G.A. Somorjai, J. Am. Chem. Soc. 102 (1980) 5494.
[11] R.G. Carr, G.A. Somorjai, Nature 290 (1981) 576.
[12] T. Kawai, T. Sakata, Chem. Phys. Lett. 70 (1980) 131.
[13] K. Domen, S. Naito, M. Soma, T. Onishi, K. Tamaru, J. Chem. Soc. Chem. Commun. (1980) 543.
[14] S. Sato, J.M. White, Chem. Phys. Lett. 72 (1980) 83.
[15] S. Sato, J.M. White, J. Catal. 69 (1981) 128.
[16] K. Yamaguchi, S. Sato, J. Chem. Soc., Faraday Trans. 1 (81) (1985) 1237.
[17] A.L. linsebigler, G. Lu, J.T. Yates, Chem. Rev. 95 (1995) 735.
[18] S. Tabata, H. Nishida, Y. Masaki, K. Tabata, Catal. Lett. 34 (1995) 245.
[19] H. Kominami, S. Murakami, M. Kohno, Y. Kera, K. Okada, B. Ohtani, Phys. Chem. Chem. Phys. 3 (2001) 4102.
[20] B. Ohtani, R. Bowman, D.P. Colombo Jr., H. Kominami, H. Noguchi, K. Uosaki, Chem. Lett. (1998) 579.
[21] K. Sayama, H. Arakawa, J. Phys. Chem. 97 (1993) 531.
[22] K. Sayama, H. Arakawa, J. Chem. Soc., Faraday Trans. 93 (1997) 1647.
[23] S.C. Moon, H. Mametsuka, E. Suzuki, Y. Nakahara, Catal. Today 45 (1998) 79.
[24] Y. Inoue, T. Niiyama, Y. Asai, K. Sato, J. Chem. Soc., Chem. Commun. (1992) 579.
[25] Y. Inoue, Y. Asai, K. Sato, J. Chem. Soc., Faraday Trans. 90 (1994) 797.
[26] K. Domen, A. Kudo, A. Shinozaki, A. Tanaka, K. Maruya, T. Onishi, J. Chem. Soc., Chem. Commun. (1986) 356.
[27] K. Domen, A. Kudo, M. Shibata, A. Tanaka, K. Maruya, T. Onishi, J. Chem. Soc., Chem. Commun. (1986) 1706.
[28] A. Kudo, A. Tanaka, K. Domen, K. Maruya, K. Aika, T. Onishi, J. Catal. 111 (1988) 67.
[29] N. Kinomura, N. Kumada, F. Muto, J. Chem. Soc. Dalton Trans. 11 (1985) 2349.
[30] H. Kato, K. Asakura, A. Kudo, J. Am. Chem. Soc. 125 (2003) 3082.
[31] H. Kato, A. Kudo, Catal. Today 78 (2003) 561.
[32] D.E. Scaife, Solar Energy 25 (1980) 41.
[33] M.R. Hoffmann, S.T. Martin, W.Y. Choi, D.W. Bahnemann, Chem. Rev. 95 (1995) 69.
[34] M. Anpo, Y. Ichihashi, M. Takeuchi, H. Yamashita, Res. Chem. Intermed. 24 (1998) 143.
[35] M. Anpo, Catal. Surv. Jpn. 1 (1997) 169.
[36] M. Anpo, M. Takeuchi, S. Kishiguchi, H. Yamashita, Surf. Sci. Jpn. 20 (1999) 60.
[37] H. Yamashita, Y. Ichihashi, M. Takeuchi, S. Kishiguchi, M. Anpo, J. Synchrotron. Rad. 6 (1999) 451.
[38] M. Anpo, Pure Appl. Chem. 72 (2000) 1265.
[39] M. Anpo, Pure Appl. Chem. 72 (2000) 1787.
[40] M. Anpo, Stud. Surf. Sci. Catal. 130 (2000) 157.
[41] H. Yamashita, M. Harada, J. Misaka, M. Takeuchi, K. Ikeue, M. Anpo, J. Photochem. Photobiol. A 148 (2002) 257.
[42] M. Anpo, M. Takeuchi, J. Catal. 216 (2003) 505.
[43] R. Niishiro, H. Kudo, A. Kudo, Phys. Chem. Chem. Phys. 7 (2005) 2241.
[44] Z. Zou, J. Ye, K. Sayama, H. Arakawa, Nature 414 (2001) 625.
[45] R. Asahi, T. Morikawa, T. Ohwaki, K. Aoki, Y. Taga, Science 293 (2001) 269.
[46] T. Morikawa, R. Asahi, T. Ohwaki, K. Aoki, Y. Taga, Jpn. J. Appl. Phys. 40 (2001) L561.
[47] T. Umebayashi, T. Yamaki, H. Itoh, K. Asai, Appl. Phys. Lett. 81 (2002) 454.
[48] T. Ohno, Z. Miyamoto, K. Nishijima, H. Kanemitsu, X.Y. Feng, Appl. Catal. A: Gen. 302 (2006) 62.
[49] S.U.M. Khan, M. Al-Shahry, W.B. Ingler Jr., Science 297 (2002) 2243.
[50] H. Irie, Y. Watanabe, K. Hashimoto, Chem. Lett. 32 (2003) 772.
[51] S. Sakthivel, H. Kisch, Angrew. Chem., Int. Ed. 42 (2003) 4908.
[52] R. Abe, T. Takata, H. Sugiharaa, K. Domen, J. Chem. Soc. Chem. Commun. (2005) 3829.
[53] K. Maeda, K. Teramura, D. Lu, T. Takata, N. Saito, Y. Inoue, K. Domen, Nature 440 (2006) 295.
[54] K. Fujihara, T. Ohno, M. Matsumura, J. Chem. Soc., Faraday Trans. 94 (1998) 3705.
[55] S.C. Moon, Y. Matsumura, M. Kitano, M. Matsuoka, M. Anpo, Res. Chem. Intermed. 29 (2003) 233.
[56] M. Anpo, Bull. Chem. Soc. Jpn. 77 (2004) 1427.
[57] M. Anpo, S. Dohshi, M. Kitano, Y. Hu, M. Takeuchi, M. Matsuoka, Annu. Rev. Mater. Res. 35 (2005) 1.
[58] M. Matsuoka, M. Kitano, M. Takeuchi, M. Anpo, J.M. Thomas, Mater. Sci. Forum 486–487 (2005) 81.
[59] M. Takeuchi, M. Anpo, T. Hirao, N. Itoh, N. Iwamoto, Surf. Sci. Jpn. 22 (2001) 561.
[60] M. Kitano, M. Takeuchi, M. Matsuoka, J.M. Thomas, M. Anpo, Chem. Lett. 34 (2005) 616.
[61] M. Matsuoka, M. Kitano, M. Takeuchi, M. Anpo, J.M. Thomas, Top. Catal. 35 (2005) 305.
[62] M. Kitano, H. Kikuchi, T. Hosoda, M. Takeuchi, M. Matsuoka, T. Eura, M. Anpo, J.M. Thomas, Key Eng. Mater. 317–318 (2006) 823.
[63] H. Kikuchi, M. Kitano, M. Takeuchi, M. Matsuoka, M. Anpo, P.V. Kamat, J. Phys. Chem. B 110 (2006) 5537.
[64] T. Torimoto, R.J. Fox, M.A. Fox, J. Electrochem. Soc. 143 (1996) 3712.
[65] D.C. Hurum, A.G. Agrios, K.A. Gray, T. Rajh, M.C. Thurnauer, J. Phys. Chem. B 107 (2003) 4545.